

5-1-2013

The function of the left angular gyrus in mental arithmetic: Evidence from the associative confusion effect

Roland H. Grabner
ETH Zürich

Daniel Ansari
Western University, daniel.ansari@uwo.ca

Karl Koschutnig
Medizinische Universität Graz

Gernot Reishofer
Medizinische Universität Graz

Franz Ebner
Medizinische Universität Graz

Follow this and additional works at: <https://ir.lib.uwo.ca/paedpub>



Part of the [Pediatrics Commons](#)

Citation of this paper:

Grabner, Roland H.; Ansari, Daniel; Koschutnig, Karl; Reishofer, Gernot; and Ebner, Franz, "The function of the left angular gyrus in mental arithmetic: Evidence from the associative confusion effect" (2013).

Paediatrics Publications. 652.

<https://ir.lib.uwo.ca/paedpub/652>

The Function of the Left Angular Gyrus in Mental Arithmetic: Evidence from the Associative Confusion Effect

Roland H. Grabner,^{1*} Daniel Ansari,² Karl Koschutnig,³ Gernot Reishofer,⁴
and Franz Ebner³

¹Research on Learning and Instruction, Institute for Behavioral Sciences, Swiss Federal Institute of Technology (ETH) Zurich, Switzerland

²Department of Psychology, Numerical Cognition Laboratory, University of Western Ontario, Canada

³Department of Radiology, Division of Neuroradiology, Medical University of Graz, Austria

⁴Department of Radiology, Division of MR Physics, Medical University of Graz, Austria

Abstract: While the left angular gyrus (IAG) has been repeatedly implicated in mental arithmetic, its precise functional role has not been established. On the one hand, it has been speculated that the IAG is involved in task-specific processes. On the other hand, the observation of relative deactivation during arithmetic has led to the contention that differential IAG activation reflects task-unrelated difficulty effects associated with the default mode network (DMN). Using functional magnetic resonance imaging, we investigated the neural correlates of the associative confusion effect that allowed us to dissociate effects of task difficulty and task-related arithmetic processes on IAG activation. The associative confusion effect is characterized by poorer performance while verifying addition and multiplication equations whose solutions are associated with the other operation (confusion equations: e.g., “ $9 \times 6 = 15$ ”) compared with solutions unrelated to both operations (non-confusion equations: e.g., “ $9 \times 6 = 52$ ”). Comparing these two conditions revealed higher activation of the anterior IAG (areas PGa, PFm, and PF) and the left dorsolateral prefrontal cortex for the confusion problems. This effect displayed only slight anatomical overlap with the well-established reverse problem-size effect (small minus large problems) and task-related deactivation in the parietal cortex. The finding of greater IAG activity (less deactivation) in the more difficult task condition is inconsistent with the hypothesis that IAG activation during mental arithmetic reflects task difficulty related modulations of the DMN. Instead, the present findings provide further support for the symbol-referent mapping hypothesis, suggesting that the IAG mediates the automatic mapping of arithmetic problems onto solutions stored in memory. *Hum Brain Mapp* 34:1013–1024, 2013. © 2011 Wiley Periodicals, Inc.

Key words: problem solving; fMRI; parietal cortex; fact retrieval; default mode network; symbol-referent mapping

Contract grant sponsor: Provincial Government of Styria (Landesregierung Steiermark) in Austria.

*Correspondence to: Roland H. Grabner, Institute for Behavioral Sciences, Swiss Federal Institute of Technology (ETH) Zurich, Universitaetsstrasse 41 UNO C15, CH-8092 Zurich, Switzerland. E-mail: grabner@ifv.gess.ethz.ch

Received for publication 25 May 2011; Accepted 16 September 2011

DOI: 10.1002/hbm.21489

Published online 29 November 2011 in Wiley Online Library (wileyonlinelibrary.com).

INTRODUCTION

There is a wealth of evidence from neuropsychological and neuroimaging studies demonstrating that the left angular gyrus (LAG) is systematically involved in mental arithmetic (Zamarian et al., 2009). The precise role played by this brain region in calculation is, however, still poorly understood. One hypothesis posits that the LAG subserves the retrieval of arithmetic facts stored in verbal memory (Dehaene et al., 2003). This hypothesis is supported by data showing that the activation of this region increases with arithmetic training (Delazer et al., 2003; Ischebeck et al., 2006), is higher while solving problems of small compared with large size (Stanescu-Cosson et al., 2000) and during problem-solving through fact retrieval compared with calculation procedures (Grabner et al., 2009a).

An alternative hypothesis (Ansari, 2008) states that the LAG supports the automatic mapping between mathematical symbols and their semantic referents, such as mappings between Arabic digits and magnitude representations or between arithmetic problems and solutions stored in memory (i.e., arithmetic facts). In arithmetic, it is assumed that overlearned arithmetic problems become higher-order symbols and that their presentation automatically activates the associated solution in long-term memory. This hypothesis of LAG function is compatible with the aforementioned neuroimaging studies of arithmetic processing but can additionally account for recent findings of LAG involvement in the processing of symbolic digits even without arithmetic demands (Holloway et al., 2010; Price and Ansari, in press).

Both hypotheses are challenged by the fact that the LAG is part of the default mode network (DMN; Raichle et al., 2001) and that its activation during mental arithmetic behaves similarly to the nodes of this network. The DMN is generally deactivated during cognitive processing compared with rest and shows stronger deactivations in more difficult tasks (Buckner et al., 2008; McKiernan et al., 2003). Also in mental arithmetic, the LAG has been found to be deactivated during task processing and to exhibit stronger deactivations in more difficult task conditions (e.g., Grabner et al., 2009b; Ischebeck et al., 2006). This is particularly evident in the so-called reverse problem-size effect in the LAG which refers to greater activation (less deactivation) in small compared with large problems (e.g., Grabner et al., 2007; Stanescu-Cosson et al., 2000). Against this background, it has been hypothesized that the LAG is unrelated to arithmetic processing and that activation dif-

ferences only reflect general effects of task difficulty (Wu et al., 2009; Zago et al., 2001).

In the present functional magnetic resonance imaging (fMRI) study, we applied a well-established behavioral paradigm that has the potential to evaluate whether the LAG involvement in mental arithmetic indeed is only an epiphenomenon of task difficulty or whether it reflects task-specific cognitive processes in terms of fact retrieval or symbol-referent mapping. Specifically, we investigated the neural correlates of the associative confusion effect (Winkelman and Schmidt, 1974) which is characterized by lower accuracy and longer response times (RTs) while verifying addition or multiplication equations whose solutions are correct in the other arithmetic operation (confusion equations: e.g., “ $9 \times 6 = 15$ ”) compared with solutions which are incorrect for either operation (non-confusion equations: e.g., “ $9 \times 6 = 52$ ”). The higher difficulty of confusion equations has been attributed to the automatic activation of (incorrect) arithmetic facts in memory and the need for further cognitive processing (Zbrodoff and Logan, 1986). If the LAG was only modulated by task difficulty, lower LAG activation (more deactivation) should emerge in the (more difficult) confusion equations. However, if the LAG supported the automatic mapping of arithmetic problems (specifically, the presented operands) and the associated solution, *higher* LAG activation (less deactivation) should occur in the confusion (compared with non-confusion) equations. The fact retrieval hypothesis, in contrast, is ambiguous with respect to its prediction of LAG involvement in confusion and non-confusion equations. On the one hand, larger activation in the confusion compared with non-confusion equations could be explained in terms of stronger reliance on fact retrieval compared with calculation. On the other hand, confusion and non-confusion equations involve problems of similar size and, thus, can be expected to equally strongly rely on fact retrieval (Campbell and Xue, 2001) and to exhibit similar LAG activation. In addition to contrasting confusion and non-confusion equations, we sought to replicate the well-established task-related deactivation (Buckner et al., 2008) and reverse problem-size effect (Stanescu-Cosson et al., 2000) in the LAG. These analyses should also reveal anatomical overlap and dissociations between the effects.

MATERIALS AND METHODS

Participants

Thirty-four adults participated in the present investigation. Due to technical problems or large movement artifacts (exceeding 2 mm between subsequent volumes), four participants had to be excluded from further analyses. The remaining sample comprised 30 adults (half males) between 19 and 29 years ($M = 22.67$, $SD = 2.60$). All participants were right-handed and had normal or corrected-to-normal vision. They gave written informed consent and were paid for their participation. The study was approved

Abbreviations

DLPFC	dorsolateral prefrontal cortex
DMN	default mode network
fMRI	functional magnetic resonance imaging
LAG	left angular gyrus
RT	response time

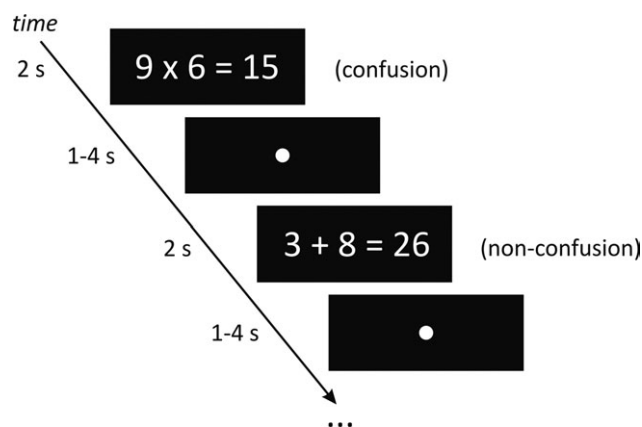


Figure 1.

Schematic display of event-related fMRI design with example items of confusion and non-confusion equations.

by the local ethics committee (Medical University of Graz, Austria).

Materials and fMRI Design

During fMRI data acquisition, participants worked on 126 addition and 126 multiplication problems with single-digit operands ranging from $2 + / \times 3$ to $9 + / \times 9$. According to the problem-size definition by Campbell and Xue (2001), about half of the problems (62 within each operation) were small (products ≤ 25), whereas the remaining problems were large (products > 25). Problem selection followed the procedure described in Lemaire et al. (1996). Tie problems (e.g., “ $3 + 3$ ”) were included. An arithmetic verification paradigm was administered in which participants were presented an equation (e.g., “ $5 + 8 = 13$ ”) and had to indicate by button press whether the given result is correct (right-hand button) or not (left-hand button). Half of the presented problems contained correct solutions (correct equations), whereas within the other half (63 addition and 63 multiplication problems) 32 problems included incorrect confusion solutions (confusion equations) and 31 problems incorrect non-confusion solutions (non-confusion equations; see Fig. 1). Confusion solutions were the correct result from the other operation, i.e., the correct addition result in a multiplication problem (e.g., “ $9 \times 6 = 15$ ”) or vice versa (e.g., “ $2 + 6 = 12$ ”). Non-confusion solutions were created by adding or subtracting 1 or 2 to or from the confusion solution. This was done to equate the difference between correct and incorrect solutions for the (incorrect) confusion and non-confusion equations, as this difference has been found to affect reaction times in arithmetic verification tasks (see Lemaire et al., 1996). For instance, the confusion equation “ $9 + 9 = 81$ ” has a large difference between correct solution (“18”) and incorrect solution (“81”).

The 252 equations of both operations were presented in an event-related fMRI design consisting of six runs with 42 problems each. Each equation was presented for 2 s, followed by an inter-trial interval of 1–4 s (jittered in 1 s steps across the problems; $M = 2.5$ s) during which a fixation point was on the screen (see Fig. 1). Addition and multiplication equations were presented intermixed to increase the confusion effect (Lemaire et al., 1991, 1994; Zbrodoff and Logan, 1986). The order of the problems was pseudorandomized. Each run started with the number of the run presented on the screen for 3 s followed by a 25 s fixation period. At the end of each run, another fixation period of 25 s was included. Before imaging was performed, the task was demonstrated to participants and any questions were answered. Instructions stressed speed and accuracy.

Data Acquisition and Analysis

Imaging was performed in a 3.0 T Tim Trio system (Siemens Medical Systems, Erlangen, Germany) using an 8-channel head coil. Functional images were obtained with a single shot gradient echo planar imaging (EPI) sequence (time to repeat (TR) = 2,000 ms, time to echo (TE) = 30 ms, flip angle (FA) = 90° , matrix size = 64×64 , slice thickness = 3 mm, spatial resolution = 3×3 mm). In total, 729 functional volumes (first two were discarded) with 31 transverse slices (3-mm thickness, 0.09-mm gap) were acquired in descending order. Stimulus presentation was accomplished with the Eloquence system (In vivo Corporation, Orlando, FL), containing an LCD display visible for the participant through a mirror mounted above the head coil. The paradigm was presented using the software package Presentation (Neurobehavioral Systems, Albany, CA).

fMRI data analysis was performed using SPM5 (Wellcome Department of Imaging Neuroscience, London, UK). The functional data of each participant were motion-corrected, slice-time corrected, spatially normalized into the standard MNI space (Montreal Neurological Institute) using a voxel size of 3 mm, and smoothed using a Gaussian kernel of 8 mm FWHM. The statistical analysis was conducted on the basis of the general linear model as implemented in SPM. Only valid (i.e., correctly solved) trials were entered into the analyses. Model time courses for each experimental condition (correct, confusion, non-confusion equations; correct equations separately for small and large problem size) and the (25 s) fixation periods (at the start and end of each run) were generated on the basis of the hemodynamic response function as given by SPM5. Invalid (i.e., incorrectly solved) trials, the time interval during the presentation of the run number, and the six motion parameters were entered into the model as regressors of no interest. A high-pass filter with a cutoff frequency of $1/256$ Hz was employed to remove low-frequency drifts. The analysis for the entire group was performed by computing linear t -contrasts for each subject

individually which were then entered into a random-effects model.

To test the research hypotheses outlined in the introduction, we contrasted confusion and non-confusion equations without and with controlling for the behavioural confusion effect. The latter analysis was conducted against the background of the discussion whether activation differences in traditional resting-state brain regions such as the IAG may solely be due to differences in task difficulty. Two control analyses were calculated. In the first analysis, we entered the normalized confusion-related RT differences (calculated as confusion RT minus non-confusion RT, divided by non-confusion RT) as covariate in the (second-level) random-effects model (one-sample t-test) contrasting confusion versus non-confusion equations. In the second analysis, we did the same with normalized confusion-related accuracy differences (calculated as non-confusion accuracy minus confusion accuracy, divided by non-confusion accuracy).

In addition to the contrast between confusion and non-confusion equations, we calculated two further comparisons. First, we contrasted the fixation periods with the experimental task intervals (fixation > task) to reveal brain areas showing task-related deactivation. This contrast served as an estimate of the task-modulated DMN, since this network shows reliably greater activation during rest compared with task (Buckner et al., 2008). Second, we contrasted small and large correct equations (i.e., equations containing the correct solutions; small > large) to reveal the well-established reverse problem-size effect in the IAG (e.g., Stanescu-Cosson et al., 2000).

Significant activation differences between confusion and non-confusion conditions were identified using an initial voxel-wise threshold of $P < 0.001$ uncorrected. Only activation clusters significant at $P < 0.05$ family-wise error (FWE) corrected for multiple comparisons at cluster level are reported. The anatomical location of the significant activation clusters was generally analysed by means of the AAL (automated anatomical labelling) atlas (Tzourio-Mazoyer et al., 2002). In addition, the left-hemispheric parietal brain regions associated with the IAG were analyzed in more detail using probabilistic cytoarchitectonic maps (Caspers et al., 2006; Eickhoff et al., 2005). These maps provide a more fine-grained parcellation of the angular gyrus (into an anterior, PGa, and posterior part, PGp) as well as of the supramarginal gyrus (into five areas: PFop, PFt, PF, PFm, and PFcm).

RESULTS

Accuracy and response latencies of the experimental conditions are depicted in Figure 2a. As expected, confusion equations were verified less accurately [$t(29) = -3.81$, $P < 0.001$] and associated with longer RTs [$t(29) = 3.45$, $P < 0.01$] than non-confusion equations. Correct equations displayed a lower accuracy than non-confusion equations

[$t(29) = -3.94$, $P < 0.001$] and shorter RTs than confusion equations [$t(29) = -3.04$, $P < 0.01$].

Analysis of the fMRI data revealed that solving confusion equations was associated with stronger (relative) activation in left middle to superior frontal cortex, corresponding to the left dorsolateral prefrontal cortex (DLPFC), and IAG extending to the supramarginal gyrus and inferior parietal cortex (Table Ia, Fig. 2b). The reverse contrast (non-confusion > confusion equations) did not yield any significant activation clusters. To evaluate whether the observed activation differences reflect differences in relative activation or deactivation, respectively, we extracted the individual contrast estimates for the confusion and non-confusion equation conditions (both against the baseline fixation periods) from the IAG and left DLPFC regions observed in the whole-brain contrast reported above. It turned out that both regions displayed relative deactivation compared with rest and that the higher activation in the confusion equations is due to less deactivation compared with the non-confusion equations (see Fig. 2b). The analyses controlling for performance differences between confusion and non-confusion equations did not change the finding of higher IAG activation in the confusion condition, neither when controlling for reaction time (see Table I) nor for accuracy (see Table I). However, in both control analyses, the activation difference in the left DLPFC diminished.

The contrast of fixation minus task revealed a widespread network of activation clusters comprising those typically observed in analyses of the DMN, including medial frontal cortices, the posterior cingulate, and, most importantly, the angular gyri bilaterally (Table II, Fig. 3a). The activation cluster overlapping with the IAG also displayed relative deactivation compared with baseline ($M = -10.25$, $SD = 8.05$).

Finally, verifying small compared with large (correct) equations was associated with stronger activation in the angular gyri and the anterior cingulate, bilaterally (see Table III and Fig. 3b). Analyses of the contrast estimates against fixation revealed that the activation differences in all three regions were due to differences in relative deactivation, similar to the associative confusion effect.

A closer look at the anatomical locations of the left parietal activation clusters related to the association confusion effect, the task-related deactivations, and the reverse problem-size effect uncovered remarkable topographical differences (see Fig. 4a): The associative confusion effect lies most anteriorly and only partly overlaps with the other two activation clusters. In terms of probabilistic cytoarchitectonic maps, more than half of this cluster is located in region PFm in the supramarginal gyrus, followed by PGa and PF (see Table IV and Fig. 2c). The task-related deactivation in the left parietal cortex, in contrast, mainly covers the PGa and PGp areas, and slightly overlaps with the associative confusion effect (Table IV). The reverse problem-size effect is mainly located in the area PGa and almost entirely overlaps with the anterior part of the task-

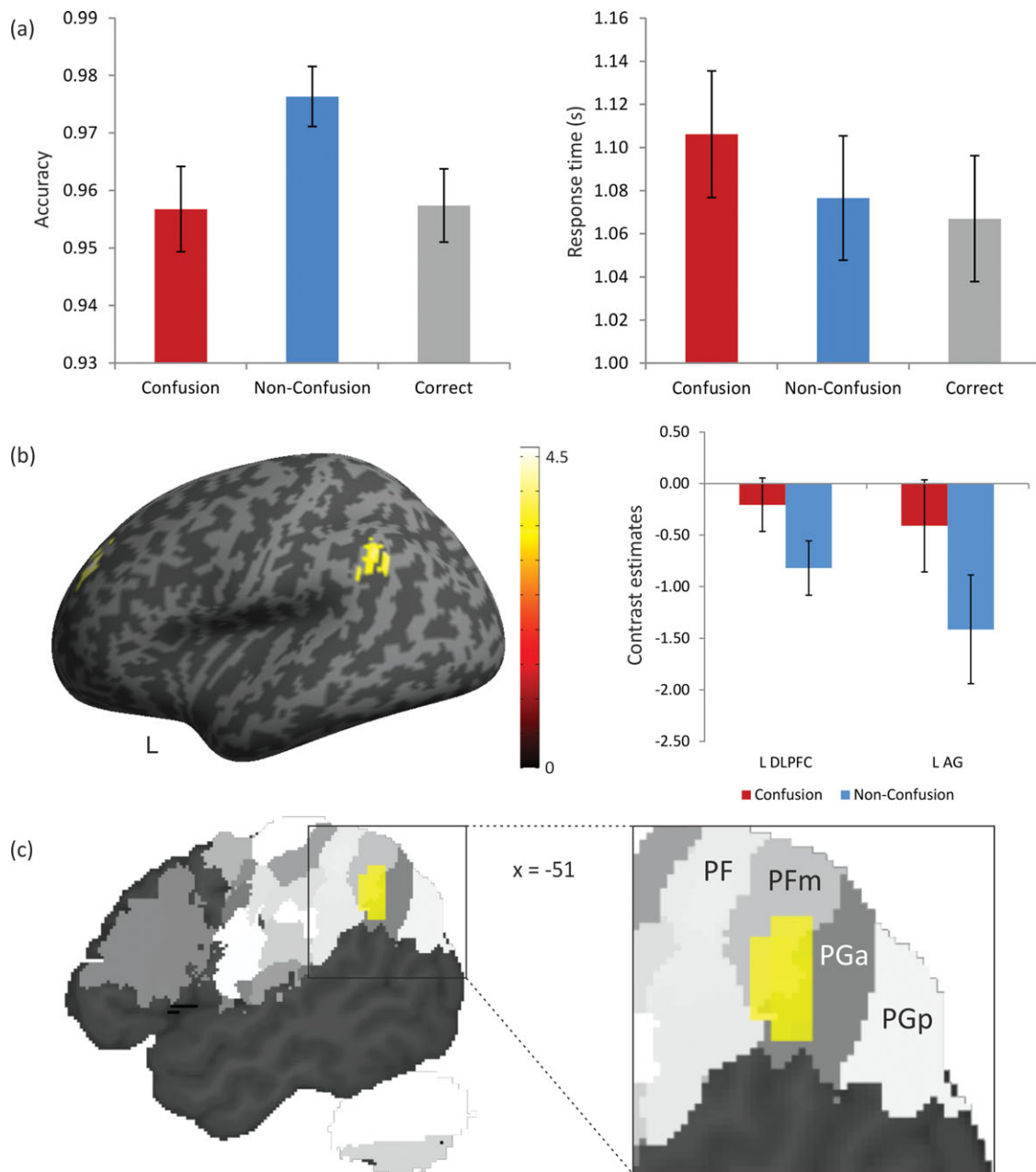


Figure 2.

Associative confusion effect. (a) Accuracy (left) and response times (right) of the experimental conditions. (b) Significant activation clusters in the contrast confusion > non-confusion equations (left) and corresponding contrast estimates against fixation (right). (c) Anatomical location of the activation cluster accord-

ing to probabilistic cytoarchitectonic maps. L = left; DLPFC = dorsolateral prefrontal cortex; AG = angular gyrus. Error bars depict ± 1 SE of the mean. [Color figure can be viewed in the online issue, which is available at wileyonlinelibrary.com.]

related deactivation cluster. Also this cluster displays only a slight overlap with the associative confusion effect (see Fig. 4a). Figure 4b depicts the contrast estimates (against fixation) of all investigated conditions for the probabilistic cytoarchitectonic areas showing significant effects in the

whole-brain contrasts. In line with previous studies on mental arithmetic (Rosenberg-Lee et al., 2011; Wu et al., 2009), the areas of the supramarginal gyrus (PF and PFm) displayed relative activation, whereas the areas of the IAG (PGa and PGp) were consistently deactivated.

TABLE I. Associative confusion effect: Overview of significant activation differences in the contrast confusion > non-confusion equations (a) without controlling for confusion-related performance differences, (b) with confusion-related differences in reaction time as covariate, (c) with confusion-related differences in accuracy as covariate

Brain region	Cluster (%)	x	y	z	k	t
(a)						
L AG	17.91	-51	-51	36	67	4.09
L iPG	41.79					
L SMG	29.85					
L mFG	43.10	-21	42	30	58	5.15
L sFG	50.00					
L med sFG	6.90					
(b)						
L AG	15.87	-51	-51	36	63	4.02
L iPG	42.86					
L SMG	31.75					
(c)						
L AG	17.74	-51	-51	36	62	4.02
L iPG	40.32					
L SMG	32.26					

Note: Coordinates refer to the activation peak of the cluster and are reported in MNI (Montreal Neurological Institute) space as given by SPM5. The anatomical localization is presented based on the AAL (automated anatomical labelling) atlas (Tzourio-Mazoyer et al., 2002). The first label denotes the location of the peak activation, further labels indicate different brain regions within the same activation cluster (including submaximal). Only activation clusters significant at $p < .05$ corrected for multiple comparisons at cluster level are reported.

Abbreviations: L = left hemisphere; R = right hemisphere; i = inferior; m = middle; med = medial; FG = frontal gyrus; PG = parietal gyrus; AG = angular gyrus; SMG = supramarginal gyrus.

DISCUSSION

Three main hypotheses on the functional significance of the IAG have been put forward. It has been argued to support the retrieval of arithmetic facts from memory (Dehaene et al., 2003), automatic mapping processes between arithmetic problems and associated solutions (Ansari, 2008), and to reflect domain-general difficulty effects and corresponding modulation of the DMN (Wu et al., 2009; Zago et al., 2001).

In this study, we sought to differentiate between these hypotheses by investigating the neural correlates of the associative confusion effect in mental arithmetic (Winkelman and Schmidt, 1974). The associative confusion paradigm provides a unique opportunity to disentangle task difficulty related processing from processes related to the retrieval of arithmetic facts or the automatic mapping between arithmetic problems and their solutions. The present findings revealed higher activity in the anterior aspect of the IAG (area PGa), extending to the supramarginal

gyrus (in particular area PFm), and left DLPFC while solving arithmetic equations with associative confusions (e.g., “ $9 \times 6 = 15$ ”) compared with non-confusion equations

TABLE II. Task-related deactivations: Overview of significant activation differences in the contrast fixation > experimental task

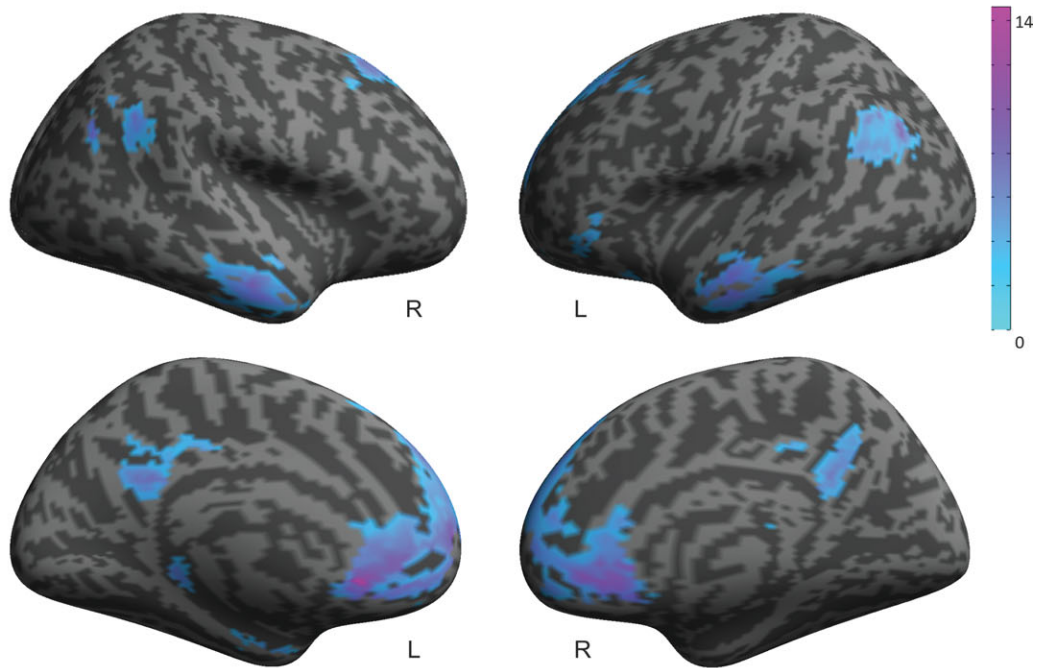
Brain region	Cluster (%)	x	y	z	k	t
L ACC	10.34	-6	24	-9	2243	14.62
L med sFG	20.82					
R med sFG	12.88					
L sFG	12.22					
R sFG	7.58					
R ACC	6.33					
L med orb FG	5.80					
R med orb FG	5.66					
L mOG	6.33	-45	-75	36	316	11.03
L AG	66.46					
L mTG	9.18					
L iPG	5.38					
R AG	59.93	51	-72	33	292	9.99
R iPG	15.41					
R SMG	9.59					
R sTG	6.16					
R iTG	33.43	60	-9	-30	350	8.91
R mTG	51.14					
R sTG	6.57					
R mTG Pole	5.71					
L PCC	20.79	-3	-48	30	303	7.80
L mCC	23.43					
R mCC	14.85					
L Precuneus	14.19					
R PCC	13.20					
R Precuneus	9.24					
L iTG	30.06	-54	-9	-24	316	7.68
L mTG	65.51					
L Hippocampus	3.97	-15	-36	15	126	7.63
R Hippocampus	8.65	21	-39	12	104	6.56
L orb iFG	76.19	-48	30	-12	84	5.19
L tri iFG	13.10					
L Parahippocampus	41.30	-24	-9	-27	46	5.18
L Hippocampus	41.30					
L Amygdala	8.70					

Note: Coordinates refer to the activation peak of the cluster and are reported in MNI (Montreal Neurological Institute) space as given by SPM5. The anatomical localization is presented based on the AAL (automated anatomical labelling) atlas (Tzourio-Mazoyer et al., 2002) The first label denotes the location of the peak activation, further labels indicate different brain regions within the same activation cluster (including submaxima) if the percentage of activated voxels within the cluster is ≥ 5.00 .

Only activation clusters significant at $p < .05$ corrected for multiple comparisons at cluster level are reported.

Abbreviations: L = left hemisphere; R = right hemisphere; med = medial; orb = orbital; tri = triangular; i = inferior; m = middle; s = superior; FG = frontal gyrus; TG = temporal gyrus; PG = parietal gyrus; OG = occipital gyrus; AG = angular gyrus; SMG = supramarginal gyrus; ACC = anterior cingulate; PCC = posterior cingulate; mCC = middle cingulate.

(a) Task-related deactivation



(b) Reverse problem size effect

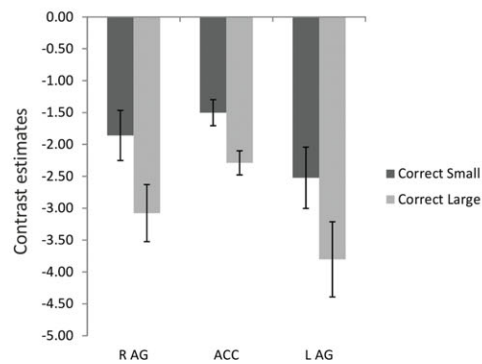
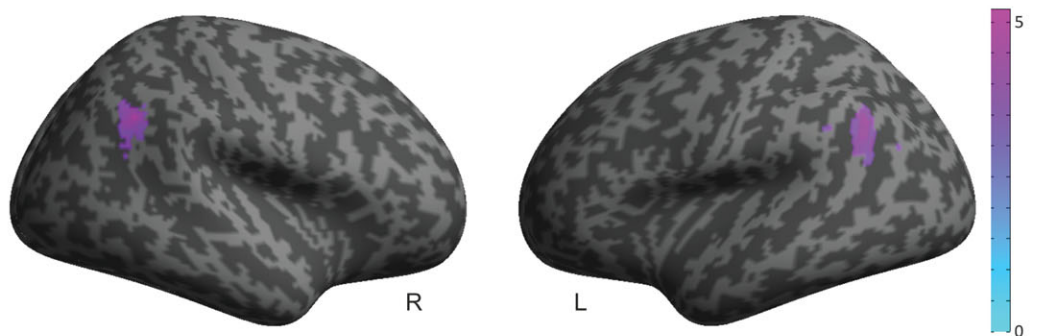


Figure 3.

(a) Task-related deactivations. Significant activation clusters in the contrast fixation > task in lateral (upper row) and medial (lower row) view. (b) Reverse problem-size effect. Significant activation clusters in the contrast small > large correct equations (upper row) and corresponding contrast estimates against

fixation (lower row). L = left, R = right, AG = angular gyrus; ACC = anterior cingulate. Error bars depict ± 1 SE of the mean. [Color figure can be viewed in the online issue, which is available at wileyonlinelibrary.com.]

TABLE III. Reverse problem-size effect: Overview of significant activation differences in the contrast small > large correct equations

Brain region	Cluster (%)	<i>x</i>	<i>y</i>	<i>z</i>	<i>k</i>	<i>t</i>
R AG	65.09	60	-57	36	169	5.66
R iPG	27.81					
L ACC	44.23	-3	24	-6	52	5.19
R ACC	21.15					
L OlfC	15.38					
R OlfC	7.69					
L AG	63.11	-57	-60	36	103	4.42
L iPG	17.48					

Notes: Coordinates refer to the activation peak of the cluster and are reported in MNI (Montreal Neurological Institute) space as given by SPM5. The anatomical localization is presented based on the AAL (automated anatomical labelling) atlas (Tzourio-Mazoyer et al., 2002) The first label denotes the location of the peak activation, further labels indicate different brain regions within the same activation cluster (including submaxima) if the percentage of activated voxels within the cluster is ≥ 5.00 .

Only activation clusters significant at $p < .05$ corrected for multiple comparisons at cluster level are reported.

Abbreviations: L = left hemisphere; R = right hemisphere; i = inferior; PG = parietal gyrus; AG = angular gyrus; ACC = anterior cingulate; OlfC = olfactory cortex.

(e.g., “ $9 \times 6 = 52$ ”). Since confusion equations were more difficult to solve than the non-confusion equations, the present demonstration of higher IAG activity in the confusion equations has important implications for the current debate about the function of the IAG in mental arithmetic. It provides the first direct evidence that the modulation of the IAG in arithmetic tasks cannot be reduced to general effects of task difficulty observed in regions of the DMN (Buckner et al., 2008; McKiernan et al., 2003; Raichle et al., 2001).

The observed positive association between IAG activity and task difficulty is contrary to the typical finding of stronger IAG deactivation in more difficult task conditions (Delazer et al., 2003; Stanesco-Cosson et al., 2000), which was also demonstrated in the reverse problem-size effect in this study. Specifically, solving large problems was associated with more deactivation in the IAG than solving small problems. In contrast, the confusion compared with non-confusion equations displayed less deactivation in the IAG. Notably, this activation difference even persisted when the behavioural difficulty effect (i.e., the associative confusion effect in terms of accuracy and RT differences) was statistically controlled for. This suggests that the modulation of IAG activity by the experimental manipulation of associative confusion is not only in the opposite direction of what would have been predicted on the basis of task difficulty hypothesis, but also unconfounded by task difficulty as estimated by reaction time and accuracy data (for similar evidence, see Rosenberg-Lee et al., 2011). Moreover, other major nodes of the DMN (e.g., the cingu-

late cortex and the ventromedial prefrontal cortex; Greicius et al., 2003) were not found not to exhibit activation differences between confusion and non-confusion equations. This finding is consistent with previous neuroimaging studies on mental arithmetic (e.g., Grabner et al., 2007, 2009b; Ischebeck et al., 2006) and, furthermore, differentiates the associative confusion from the reverse problem-size effect as the latter additionally engaged the right angular gyrus and the anterior cingulate, bilaterally. Taken together, our results demonstrating a dissociation of task difficulty and arithmetic processes rule out DMN-related explanations of differential IAG activation during calculation and, in this vein, shed new light on existing data showing modulation of IAG activation in conditions where task difficulty was confounded with arithmetic processing, such as in the comparison of small (easy) and large (difficult) problems (Stanesco-Cosson et al., 2000).

The observed activation difference between confusion and non-confusion equations also provides new insights into the functional role of the IAG in mental arithmetic. We contend that the present results can be more easily reconciled with the symbol-referent mapping hypothesis compared with the fact retrieval account. According to the first, the IAG would support mapping processes between mathematical symbols and their semantic referents stored in memory, including mappings between acquired chunks of symbols such as digits in arithmetic problems and their solutions (Ansari, 2008). In other words, arithmetic problems that are overlearned and whose solutions need no longer to be calculated (such as simple addition and multiplication problems; Campbell and Xue, 2001) would become (higher order) symbols which automatically activate the stored solutions in memory. This prediction matches very well with the account provided to explain the associative confusion effect.

In their seminal study, Winkelman and Schmidt (1974) argued that the associative confusion effect results from strong associations between pairs of digits (i.e., the operands) and their sums and products, and that the presentation of a confusion equation would activate the associated information, which interferes with the correct solution. Further behavioural experiments by Zbrodoff and Logan (1986) have shown that this activation occurs automatically and unintentionally. Following this line of argument, the mapping process should be more strongly pronounced in the confusion equations (in which operands are associated with solutions) than in the non-confusion equations and be reflected in stronger IAG activity in the first task condition. This was indeed the case in this study and provides further support for the symbol-referent mapping hypothesis. The verbal fact retrieval hypothesis, in contrast, is agnostic with respect to the automatic activation of arithmetic knowledge upon problem presentation and, therefore, does not make clear predictions for the associative confusion effect. It certainly predicts activation differences between conditions differentially relying on fact retrieval compared with calculation (such as between small and

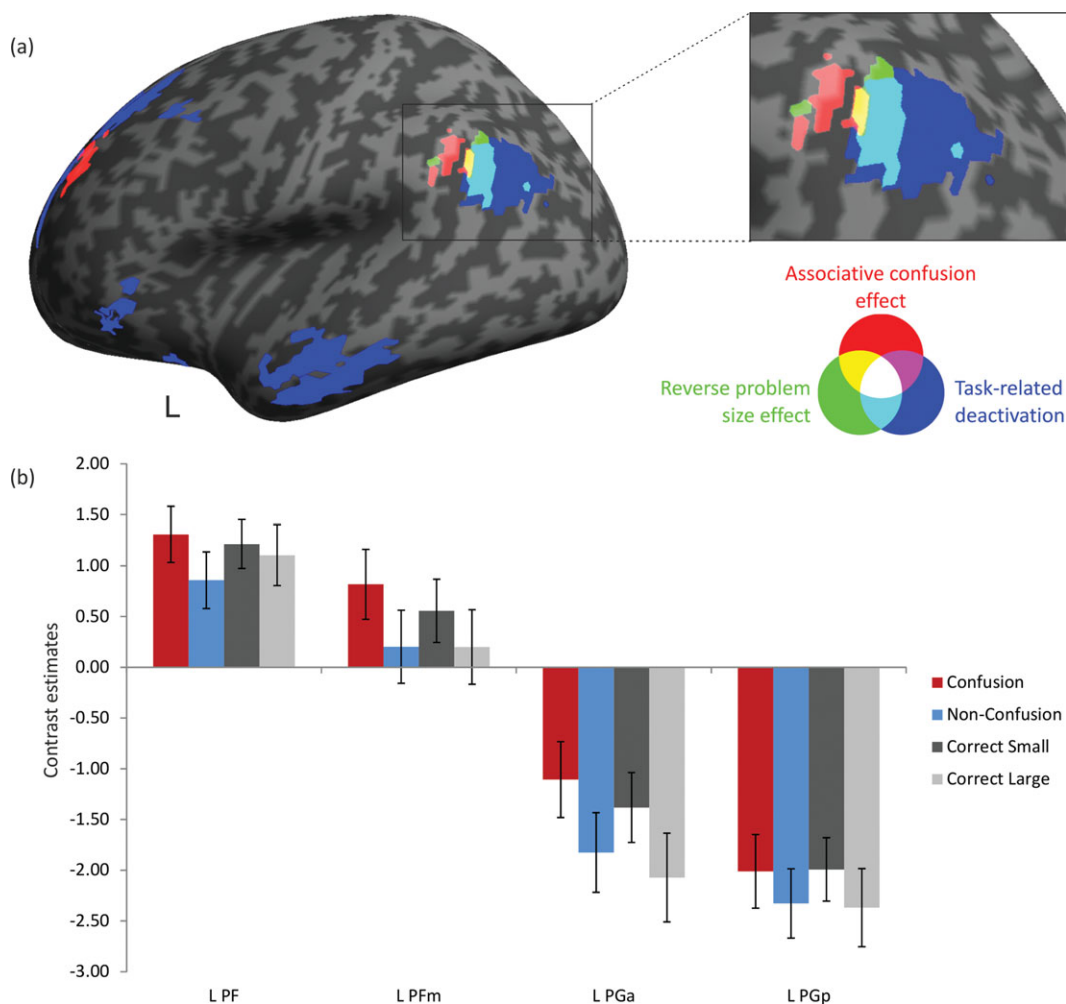


Figure 4.

(a) Conjunction display of significant activation clusters related to the associative confusion effect (red), the reverse problem-size effect (green), and the task-related deactivation (blue). Brain regions showing overlap are depicted following the additive colour model. (b) Contrast estimates against fixation of all investi-

gated conditions in anatomically defined probabilistic cytoarchitectonic regions. Error bars depict ± 1 SE of the mean. L = left. [Color figure can be viewed in the online issue, which is available at wileyonlinelibrary.com.]

large problems, as also reflected in the reverse problem-size effect) but it is unlikely that such a difference in the solution strategy exists between the confusion and non-confusion equations. Both were matched with respect to problem size and can be expected to rely on fact retrieval to a similar extent (Campbell and Xue, 2001). Thus, the observed IAG activation difference cannot be easily accounted for by this hypothesis. However, further studies are needed in which the fact retrieval and the symbol-referent mapping hypothesis are directly tested against each other.

The symbol-referent mapping hypothesis of IAG function in mental arithmetic is consistent with current views of the IAG being critically involved in semantic information processing (Binder et al., 2009; Price, 2010) and mem-

ory-related attentional processes (Cabeza et al., 2008; Ciaramelli et al., 2008).

First, there is increasing consensus that the IAG supports semantic information processing, in particular semantic information integration and knowledge retrieval (Binder et al., 2009). Recently, Seghier et al. (2010) revealed that the semantic network in the IAG partly overlaps with the DMN. The middle part of the IAG (corresponding to the area PGp) was found to intersect the DMN, whereas ventral and dorsal regions (area PGa) were exclusively modulated by semantic demands. The present findings also resemble this anatomical segregation of IAG functions. The contrast of fixation minus task revealed an activation cluster that covered the middle part (PGp) but also extended to the dorsal part (PGa) of the IAG. The

TABLE IV. Probabilistic cytoarchitectonic localization of left-hemispheric parietal brain regions for (a) the associative confusion effect, (b) task-related deactivations, and (c) the reverse problem-size effect

Brain region	Activated region (%)	Cluster (%)	Peak Probability (%)	<i>x</i>	<i>y</i>	<i>z</i>
(a)						
PFm	25.10	56.20	50	-51	-51	36
PGa	7.50	27.50	40			
PF	2.70	11.70	40			
(b)						
PGp	39.50	40.20	70	-45	-75	36
PGa	43.40	33.70	20			
PFm	10.80	5.10				
(c)						
PGa	23.70	56.60	60	-57	-60	36
PFm	13.90	20.20	50			
PGp	4.20	13.00	20			

Note: Coordinates refer to the activation peak of the cluster and are reported in MNI (Montreal Neurological Institute) space as given by SPM5. The anatomical localization is presented based on the probabilistic cytoarchitectonic maps from the SPM Anatomy toolbox (Eickhoff et al., 2005). The first label denotes the (probabilistic) location of the peak activation, further labels indicate different brain regions within the same activation cluster (including submaxima) if the percentage of activated voxels within the cluster is ≥ 5.00 . In addition, percentage of activation within the region, percentage of cluster within the region, and the probability of the peak being in the region are shown. Only activation clusters significant at $p < .05$ corrected for multiple comparisons at cluster level are reported.

activation cluster related to the associative confusion effect, in contrast, was located in the dorsal IAG (area PGa), extending to the supramarginal gyrus (PFm). According to Seghier et al., this dorsal IAG region is involved in semantic memory search, which is a process that is likely engaged during symbol-referent mapping in arithmetic problem-solving.

Second, the ventral parietal cortex covering the IAG and the supramarginal gyrus has been hypothesized to mediate bottom-up attentional processes in direct memory retrieval (Cabeza et al., 2008). Such bottom-up attentional processes occur, for instance, when a match is perceived between an external cue (e.g., an arithmetic problem) and the information stored in memory (e.g., the arithmetic fact), similar to target detection processes in perceptual tasks. Top-down attentional processes engaged in retrieval after strategic, controlled memory research, in contrast, have been linked to areas of the dorsal (superior) parietal lobe (centred on the intraparietal sulcus). This view has been supported by findings of higher inferior parietal activation for items that were recognized with high compared with low confidence (Chua et al., 2006), for strong compared with weak memories (Shannon and Buckner, 2004), and for memory retrieval facilitated by semantic priming

(Whitney et al., 2009). The present finding of higher activation in the IAG and supramarginal gyrus while solving the confusion equations adds to this line of evidence and suggests the engagement of bottom-up processes of retrieval of semantic information from memory.

Consistent with Seghier et al. (2010), the present findings draw attention to the importance of differentiating between subregions of the IAG and their functions during, on the one hand, task-specific processing such as symbol-referent mapping and, on the other hand, task-general functions such as task difficulty induced deactivation. The findings show that the associative confusion effect in the IAG and supramarginal gyrus only slightly overlaps with the general task-related deactivation and the reverse problem-size effect. The reverse problem-size effect, in contrast, largely overlaps with the task-related deactivation. In view of this, one might argue that the associative confusion contrast isolates more task-specific processes that are mediated by anterior regions of the IAG, whereas the reverse problem-size contrast identifies a mix of general processes related to differences in task difficulty and task-specific processes such as symbol-referent mapping.

Even though the present findings provide evidence that the IAG plays a functional role in mental arithmetic, it is still unclear why this brain region was, similar to many other studies (e.g., Grabner et al., 2009b; Ischebeck et al., 2006), again found to be deactivated compared with baseline. Based on findings of temporo-parietal deactivation during visual memory search (Shulman et al., 2007), Holloway et al. (2010) recently suggested that this deactivation may reflect a filter mechanism that is engaged whenever symbols cannot be mapped onto their semantic referents to allow for alternative processing. In mental arithmetic, this filter could be engaged when arithmetic knowledge is entirely lacking so that problems need to be solved by means of calculation rather than fact retrieval. Moreover, the engagement of this filter may vary as a function of the connection strength between symbols and referents. If the connections between operands and solution are weak, such as in the non-confusion equations, the filter may be more strongly activated than in arithmetic equations with strong associations between operands and solution, such as in the confusion equations. Thus, it may be tentatively speculated that a differential engagement of a filter mechanism may underlie the observed IAG deactivation difference between confusion and non-confusion equations. However, since the reverse contrast (non-confusion > confusion equations) did not yield significant activation clusters, it remains elusive what alternative processing takes place if this filter is engaged.

In addition to higher IAG activity, solving associative confusion equations was accompanied by greater activation in the left DLPFC. This finding is consistent with the view that the automatic activation of associations between operands and solutions interferes with the correct resolution and requires further cognitive control processes to select the correct solution (Lemaire et al., 1996; Zbrodoff

and Logan, 1986). A large number of studies have implicated the DLPFC in cognitive control, in general, and in conflict resolution, in particular (for reviews, cf. Fletcher and Henson, 2001; Smith and Jonides, 2003). In contrast to the anterior cingulate cortex, which has been associated with the detection of cognitive conflicts, the DLPFC has been argued to play the predominant role in the resolution of cognitive conflicts by implementing top-down attentional control (Badre and Wagner, 2004; Mansouri et al., 2007; Milham et al., 2003). Our findings thus suggest that the bottom-up attentional processes related to the automatic activation of the associated solution are complemented by top-down attentional control inhibiting the incorrect solution and adjusting the response. However, it is important to note that the activation cluster in the DLPFC did no longer reach significance when we statistically controlled for the difference in task difficulty between confusion and non-confusion equations. This suggests that this brain region may be more affected by difficulty effects than the IAG.

In conclusion, the present findings are the first to demonstrate a functional role of the IAG in mental arithmetic and rule out the current account that activation differences in the IAG related to arithmetic demands are an epiphenomenon of task difficulty effects in the DMN. In particular, the results suggest that the IAG supports automatic mappings between mathematical symbols (arithmetic problems) and semantic referents (solutions in stored in long-term memory).

REFERENCES

- Ansari D (2008): Effects of development and enculturation on number representation in the brain. *Nat Rev Neurosci* 9:278–291.
- Badre D, Wagner AD. (2004): Selection, integration, and conflict monitoring: Assessing the nature and generality of prefrontal cognitive control mechanisms. *Neuron* 41:473–487.
- Binder JR, Desai RH, Graves WW, Conant LL (2009): Where is the semantic system? A critical review and meta-analysis of 120 functional neuroimaging studies. *Cereb Cortex* 19:2767–2796.
- Buckner RL, Andrews-Hanna JR, Schacter DL (2008). The brain's default network—atomy, function, and relevance to disease. *Ann N Y Acad Sci* 1124:1–38.
- Cabeza R, Ciaramelli E, Olson IR, Moscovitch M (2008): The parietal cortex and episodic memory: an attentional account. *Nat Rev Neurosci* 9:613–625.
- Campbell JID, Xue QL (2001): Cognitive arithmetic across cultures. *J Exp Psychol Gen* 130:299–315.
- Caspers S, Geyer S, Schleicher A, Mohlberg H, Amunts K, Zilles K (2006): The human inferior parietal cortex: cytoarchitectonic parcellation and interindividual variability. *NeuroImage* 33:430–448.
- Chua EF, Schacter DL, Rand-Glovannetti E, Sperling RA (2006): Understanding metamemory: neural correlates of the cognitive process and subjective level of confidence in recognition memory. *NeuroImage* 29:1150–1160.
- Ciaramelli E, Grady CL, Moscovitch M (2008): Top-down and bottom-up attention to memory: a hypothesis (AtoM) on the role of the posterior parietal cortex in memory retrieval. *Neuropsychologia* 46:1828–1851.
- Dehaene S, Piazza M, Pinel P, Cohen L (2003): Three parietal circuits for number processing. *Cogn Neuropsychol* 20:487–506.
- Delazer M, Domahs F, Bartha L, Brenneis C, Lochy A, Trieb T, Benke T (2003): Learning complex arithmetic—an fMRI study. *Cogn Brain Res* 18:76–88.
- Eickhoff SB, Stephan KE, Mohlberg H, Grefkes C, Fink GR, Amunts K, Zilles K (2005): A new SPM toolbox for combining probabilistic cytoarchitectonic maps and functional imaging data. *NeuroImage* 25:1325–1335.
- Fletcher PC, Henson RNA (2001): Frontal lobes and human memory—insights from functional neuroimaging. *Brain* 124:849–881.
- Grabner RH, Ansari D, Reishofer G, Stern E, Ebner F, Neuper C (2007): Individual differences in mathematical competence predict parietal brain activation during mental calculation. *NeuroImage* 38:346–356.
- Grabner RH, Ansari D, Koschutnig K, Reishofer G, Ebner F, Neuper C (2009a) To retrieve or to calculate? Left angular gyrus mediates the retrieval of arithmetic facts during problem solving. *Neuropsychologia* 47:604–608.
- Grabner RH, Ischebeck A, Reishofer G, Koschutnig K, Delazer M, Ebner F, Neuper C (2009b) Fact learning in complex arithmetic and figural-spatial tasks: the role of the angular gyrus and its relation to mathematical competence. *Hum Brain Mapp* 30:2936–2952.
- Greicius MD, Krasnow B, Reiss AL, Menon V (2003): Functional connectivity in the resting brain: a network analysis of the default mode hypothesis. *Proc Natl Acad Sci U S A* 100:253–258.
- Holloway ID, Price GR, Ansari D (2010): Common and segregated neural pathways for the processing of symbolic and nonsymbolic numerical magnitude: an fMRI study. *NeuroImage* 49:1006–1017.
- Ischebeck A, Zamarian L, Siedentopf C, Koppelstatter F, Benke T, Felber S, Delazer M (2006): How specifically do we learn? Imaging the learning of multiplication and subtraction. *NeuroImage* 30:1365–1375.
- Lemaire P, Fayol M, Abdi H (1991): Associative confusion effect in cognitive arithmetic: evidence for partially autonomous processes. *Eur Bull Cogn Psychol* 11:587–604.
- Lemaire P, Barrett SE, Fayol M, Abdi H (1994): Automatic activation of addition and multiplication facts in elementary school children. *J Exp Child Psychol* 57:224–258.
- Lemaire P, Abdi H, Fayol M (1996): The role of working memory resources in simple cognitive arithmetic. *Eur J Cogn Psychol* 8:73–103.
- Mansouri FA, Buckley MJ, Tanaka K (2007): Mnemonic function of the dorsolateral prefrontal cortex in conflict-induced behavioral adjustment. *Science* 318:987–990.
- McKiernan KA, Kaufman JN, Kucera-Thompson J, Binder JR (2003): A parametric manipulation of factors affecting task-induced deactivation in functional neuroimaging. *J Cogn Neurosci* 15:394–408.
- Milham MP, Banich MT, Claus ED, Cohen NJ (2003): Practice-related effects demonstrate complementary roles of anterior cingulate and prefrontal cortices in attentional control. *NeuroImage* 18:483–493.
- Price CJ (2010): The anatomy of language: a review of 100 fMRI studies published in 2009. *Ann N Y Acad Sci* 1191:62–88.

- Price GR, Ansari D (2011): Symbol processing in the left angular gyrus: evidence from passive perception of digits. *NeuroImage* 57(3), 1205–1211.
- Raichle ME, MacLeod AM, Snyder AZ, Powers WJ, Gusnard DA, Shulman GL (2001): A default mode of brain function. *Proc Natl Acad Sci U S A* 98:676–682.
- Rosenberg-Lee M, Chang TT, Young CB, Wu S, Menon V (2011): Functional dissociations between four basic arithmetic operations in the human posterior parietal cortex: a cytoarchitectonic mapping study. *Neuropsychologia* 49:2592–2608.
- Seghier ML, Fagan E, Price CJ (2010): Functional subdivisions in the left angular gyrus where the semantic system meets and diverges from the default network. *J Neurosci* 30:16809–16817.
- Shannon BJ, Buckner RL (2004): Functional-anatomic correlates of memory retrieval that suggest nontraditional processing roles for multiple distinct regions within posterior parietal cortex. *J Neurosci* 24:10084–10092.
- Shulman GL, Astafiev SV, Mcavoy MP, Davossa G, Corbetta M (2007): Right Tpj deactivation during visual search: functional significance and support for a filter hypothesis. *Cerebral Cortex* 17:2625–2633.
- Smith EE, Jonides J. 2003. Executive control and thought. In: Squire LR, Bloom FE, S. K. M, Roberts JL, Spitzer NC, Zigmond MJ, editors. *Fundamental Neuroscience*, 2nd ed. San Diego, CA: Academic Press. pp 1377–1394.
- Stanescu-Cosson R, Pinel P, Van De Moortele PF, Le Bihan D, Cohen L, Dehaene S (2000): Understanding dissociations in dyscalculia—a brain imaging study of the impact of number size on the cerebral networks for exact and approximate calculation. *Brain* 123:2240–2255.
- Tzourio-Mazoyer N, Landeau B, Papathanassiou D, Crivello F, Etard O, Delcroix N, Mazoyer B, Joliot M (2002): Automated anatomical labeling of activations in SPM using a macroscopic anatomical parcellation of the MNI MRI single-subject brain. *NeuroImage* 15:273–289.
- Whitney C, Grossman M, Kircher TTJ (2009): The influence of multiple primes on bottom-up and top-down regulation during meaning retrieval: evidence for 2 distinct neural networks. *Cereb Cortex* 19:2548–2560.
- Winkelman JH, Schmidt J (1974): Associative confusions in mental arithmetic. *J Exp Psychol* 102:734–736.
- Wu SS, Chang TT, Majid A, Caspers S, Eickhoff SB, Menon V (2009): Functional heterogeneity of inferior parietal cortex during mathematical cognition assessed with cytoarchitectonic probability maps. *Cereb Cortex* 19:2930–2945.
- Zago L, Pesenti M, Mellet E, Crivello F, Mazoyer B, Tzourio-Mazoyer N (2001): Neural correlates of simple and complex mental calculation. *NeuroImage* 13:314–327.
- Zamarian L, Ischebeck A, Delazer M (2009): Neuroscience of learning arithmetic—evidence from brain imaging studies. *Neurosci Biobehav Rev* 33:909–925.
- Zbrodoff NJ, Logan GD (1986): On the autonomy of mental processes: a case study of arithmetic. *J Exp Psychol Gen* 115:118–130.